Virus Research 260 (2019) 78–85

Contents lists available at ScienceDirect

Virus Research

journal homepage: www.elsevier.com/locate/virusres

Investigation of nervous necrosis virus (NNV) replication *in vitro* using RNA *in situ* hybridization

Jae-Ok Kim, Wi-Sik Kim, Myung-Joo Oh*

Department of Aqualife Medicine, Chonnam National University, Yeosu, Republic of Korea

ARTICLE INFO

Keywords:
Nervous necrosis virus (NNV)
NNV replication status
In situ hybridization (ISH)
Double labeling ISH
Immunocytochemistry (ICC)

ABSTRACT

Nervous necrosis virus (NNV) belongs to the genus *Betanodavirus* of family *Nodaviridae*. Its genome consists of two RNA segments, RNA1 and RNA2. Several studies have investigated NNV detection by *in situ* hybridization (ISH), but these have typically focused on the detection of the RNA2 gene. In this study, we localized both RNA1 and RNA2 NNV segments in viral-infected cells by ISH, using labeled RNA probes (RNA-ISH). Also, immunocytochemistry (ICC) assay was carried out for localization of viral particle by targeting the coat protein. Further, viral quantification assays were performed by quantitative RT-PCR and viral infectivity ($TCID_{50}$) in SSN-1 cells. Viral segments were observed by RNA-ISH at 6 h post infection (hpi), while NNV particles were detected at 24 hpi by ICC. Use of double labeling RNA-ISH revealed the co-expression of the two viral segments in the same area of the cells, while RNA1 was also detected separately. Comparison of the level of viral genomic segments and viral infectivity revealed significantly more copies of RNA1 at each time points than copies of RNA2 and greater NNV titers. The results suggest that RNA1 might be expressed in the early stages of replication, with RNA2 expressed later. The virions then assemble through initially expressed viral genomic segments. Even though infectious particles displayed very efficient packaging, the RNA1 segment was still over-produced.

1. Introduction

Nervous necrosis virus (NNV), the causative agent of viral nervous necrosis (VNN)/viral encephalopathy and retinopathy (VER) affects over 120 species of cultured marine and freshwater fishes worldwide (Costa and Thompson, 2016). NNV infection normally affects larval and juvenile stages of fishes. However, mortalities have also been reported in NNV-infected adult fish (Nakai et al., 2009). NNV infection is pathologically characterized by vauolation and necrosis of brain, retina, and spinal cord (Munday et al., 2002).

NNV belongs to the genus *Betanodavirus* of family *Nodaviridae*. NNV is a non-enveloped icosahedral virus with a diameter of 25 nm. Its genome consists of two single stranded positive-sense RNA that are designated RNA1 and RNA2 (Mori et al., 1992). RNA1 (3.1 kb in length) encodes an RNA dependent RNA polymerase (RdRp) and a sub-genomic transcript of this segment named RNA3 encodes B2 protein (Sommerset and Nerland, 2004; Mézeth et al., 2009). RNA2 (1.4 kb) encrypts a viral capsid protein. Based on the T4 region sequence within RNA2, *Betanodavirus* has four genotypes: striped jack nervous necrosis virus (SJNNV), red spotted grouper nervous necrosis virus (RGNNV), barfin flounder nervous necrosis virus (BFNNV), and tiger puffer nervous necrosis virus (TPNNV) (Nishizawa et al., 1995). Johansen et al., (2004) suggested that new nodavirus isolates from turbot (*Scophalmus maximus*) belong to the fifth genotype. More recently, Olveira et al., (2009) reported the presence of reassortment between RGNNV and SJNNV.

Quantitative RT-PCR (qRT-PCR), *in situ* hybridization (ISH), and immunohistochemistry (IHC) have been used to detect *Betanodavirus* from organs and tissues of various fish species (Comps et al., 1996; Chi et al., 2001; Grove et al., 2006; Cha et al., 2007; Nopadon et al., 2009; David et al., 2010; Lopez-Jimena et al., 2011; Kim et al., 2018a, b). However, viral replication and underlying mechanism of infection with the host has not yet fully understood. Isolating fish viruses from cell culture is still used to determine pathogenic or infective viral particles. Virological diagnosis is normally based on cell isolation followed by confirmation using molecular techniques (Rodriguez Saint-Jean et al., 2003). This process can help explain the mechanism of infection and the stage of viral particle assembly.

ISH has various advantages, such as the ability to study the expression and replication of viral segments, and the localization of target sequences at the cellular level (Kumar, 2010). NNV detection using ISH has been explored in several studies, which have tended to focus RNA2 segments. Our group recently reported that RNA1 copy numbers are higher than RNA2 in nervous and non-nervous tissues in infected sevenband grouper using qRT-PCR (Kim et al., 2018b). We suggested that

* Corresponding author.
E-mail address: ohmj@jnu.ac.kr (M.-J. Oh).

https://doi.org/10.1016/j.virusres.2018.11.011
Received 17 September 2018; Received in revised form 15 November 2018; Accepted 21 November 2018
Available online 22 November 2018
0168-1702/

the RNA1 segment might play a vital role in various steps of virion synthesis. The suggestion has remained speculative in the absence of data concerning the process of RNA1 replication.

To explain the NNV replication in a fish cell line, we used RNA probes to label the RNA1 and RNA2 viral segments. ISH was performed and the viral particles were detected using by immunocytochemistry (ICC) following time dependent manner in the NNV-infected cells. In addition, we also investigated the levels of viral genome and viral infectivity in the cells to elucidate the expression pattern of both viral genomic segments as well as viral assembly processes.

2. Materials and methods

2.1. Virus and cell culture

NNV (SGYeosu08 strain, RGNNV genotype; Kim et al., 2014) was propagated in SSN-1 cells (Frerichs et al., 1996). Cells were grown in 75 cm^2 tissues culture flasks (Corning) at 25 °C and maintained with Leibovitz`s L-15 medium (Gibco) supplemented with 10% fetal bovine serum (FBS; Atlas), 100 IU/mL penicillin G (Gibco), and 100 μg/mL streptomycin (Gibco).

Virus was inoculated onto cells and the cell cultures were incubated at 25 °C until extensive complete cytopathic effect (CPE) was observed. Supernatants were harvested and centrifuged (3500 × g, 15 min 4 °C) to remove cell debris. Viral stock samples were titrate and stored at –80 °C until used. NNV titration was performed in 96-well plates (Nunc Thermo Scientific) of cultured SSN-1 cells. Ten-fold diluted virus (10^{-1} to 10^{-8}) was inoculated into well of 96-well plates and 50% tissue culture infection dose ($TCID_{50}$) was determined using the methodology described by Reed and Muench (1938) based on the number of wells displaying viral CPE.

2.2. Experimental design

SSN-1 cells were incubated at 25 °C on 16 four-well cell culture slide (SPL Life Sciences) until growth was confluent. NNV was inoculated at a multiplicity of infection (MOI) of 1.0. The inoculated cells were collected at 3, 6, 12, 24, 36, 48, 60, and 72 h post inoculation (hpi) from two culture slides to detect and localize NNV. The supernatant was removed from each cell culture slide and the adherent cells were fixed with 4% formalin solution (Junsei) for 20 min. The slides were rinsed with diethyl pyrocarbonate (DEPC; Bioneer) and maintained in 100% methanol (Sigma-Aldrich) at –20 °C until used for ISH and ICC analyses. For other slides, the supernatants were removed and adherent cells washed once with DEPC. The cells were then scraped off each of the culture slides and suspended in L-15 medium. The cells were used for quantification analysis of RNA1 and RNA2 by qRT-PCR and the remaining cells were used for viral titration on SSN-1 cells.

2.3. NNV detection by qRT-PCR

Viral RNA was extracted using an RNeasy Mini Kit (Qiagen) and cDNA synthesis using ReverTra Ace qPCR RT Kit (Toyobo) according to the manufacture`s protocols. The reaction mixture contained 1 μg total RNA and 0.1 pmol/μL of RNA1 (qNNV.R1.rev) or RNA2 (qNNV.R2.rev) reverse primers (Table 1) in a final reaction volume of 10 μL. NNV segments were detected and quantified in absolute numbers following the protocol (including specific primers) previously described by Kim et al. (2018b). One microliter of cDNA were added to a mixture (final volume of 20 μL) consisting of AccuPower 2X GreenStar qPCR Master Mix (Bioneer) and each primer set. Amplifications were carried out in duplicate for each sample using an Exicycler 96 Real-Time Quantitative Thermal Block (Bioneer) and the following parameters: initial pre-denaturation at 95 °C for 10 min, followed 40 cycles at 95 °C for 20 s and at 58 °C for 40 s. The qRT-PCR reaction specification was analyzed by melting curve analysis: in increments of 1 °C from 60 °C to 94 °C and a cooling step. The data were analyzed automatically using Exicycler Analysis software (Bioneer) and result was expressed as a count of copies per mL. Statistical analysis on the data was performed using two-way analysis of variance (ANOVA) with Bonferroni post hoc test in GraphPad Prism 5.0 software.

2.4. RNA probe labeling

Two primers pairs ISH.R1.for/ISH.R1.rev (RNA1) and ISH.R2.for/ISH.R2.rev (RNA2) (Table 1) were used as described previously by Kim et al. (2018a). The cDNA were amplified by PCR using Ex Taq (TaKaRa) following the manufacturer`s instructions. The products were subcloned into the pCRII-Topo vector (Invitrogen) with T7 promoters for *in vitro* RNA transcription. Plasmid clones were linearized with enzyme that cut the vector (Sac I) and then used as templates for antisense probe synthesis by T7 RNA polymerase. *In vitro* transcription was performed with 1 μg of linearized plasmid using either Fluorescein-12-UTR (Fluorescein) RNA (for RNA1) or Digoxigenin-11-dUTP (DIG) RNA (for RNA2) Labeling Kits (Roche) according to the manufacturer`s protocols.

2.5. RNA in situ hybridization (RNA-ISH)

Formalin-fixed cells from culture slides were rehydrated with methanol and treated with proteinase K (10 μg/mL in DEPC treated H_2O) (Roche) at room temperature (20–23 °C) for 10 min. Slides were post-fixed in 4% formaldehyde for 10 min and washed three times with phosphate buffered saline with 0.1% Tween-20 (PBST). Afterwards, slides were hybridized with hybridization mixture of 50% deionized formamide, 5× saline sodium citrate buffer (SSC), 0.1% Tween-20, 50 μg/mL heparin sodium salt (Sigma-Aldrich), 500 μg/mL transfer RNA (Sigma-Aldrich) and 0.1% 1 M critic acid containing 100–150 ng/mL of labeled RNA probe. Hybridization was performed by incubating at 65 °C over 18 h (typically overnight) in a humid chamber. Following the hybridization step, slides were washed twice (10 min each) in a 70% hybridization mixture (without heparin, transfer RNA and RNA probe) with 30% 2 × SSC at 65 °C, twice (10 min each) with 0.2 × SSC at 37 °C, and once with maleic acid buffer with 0.1% Tween-20 (MABT) for 10 min at room temperature. After washing, slides were incubated in 10% blocking solution (Roche) for 10 min at room temperature. Linked probes were detected with either anti-DIG IgG Fab fragments or anti-fluorescein IgG Fab fragments conjugated with alkaline phosphatase (AP) (Roche) in MABT at a dilution of 1:5000 at 4 °C overnight. After six washes in MABT to remove unbound Fab fragments from the slides, antibody was stained using either NBT/BCIP (Roche) or INT/BCIP (Roche) following the manufacturer's instructions. Once desired color development was observed the reaction was stopped with stop solution (10 mM Tris − HCl, pH 9.5, 1 mM EDTA, pH 8.0). Stained cells slides were then examined and photographed using a model BX53 microscope (Olympus) at magnifications up to 1000×.

2.6. Double labeling RNA-ISH

To visualize the expression of both viral RNAs on one slide, two probes were hybridized. When slides were used for hybridization, the mixture with labeled fluorescein and DIG-RNA probes was hybridized onto each slide as described above. For staining, we first used AP conjugated anti-DIG followed by staining with NBT/BCIP. After the staining step, anti-DIG was removed by incubating with 0.1 M glycine (pH 2.2) for 10 min at room temperature. Slides were washed with PBST four times (5 min each) and blocked using blocking solution as described above followed by subsequent detection with AP conjugated anti-fluorescein. The second staining was carried out using INT/BCIP. After stopping the coloration reaction, slides were washed and mounted as described above. INT/BCIP is alcohol soluble and so could be removed during processing. Therefore, we used INT/BCIP staining in the second step to obtain a similar intensity of the two colors.

Table 1
List of primers used in this study.

Usage	Primer name	Sequences (5`–3`)	Product size (bases)	Position
Quantitative PCR	qNNV.R1.for	TGGCGATCTTGCTCGTCATT	155	1235-1255
	qNNV.R1.rev	TTGTGGCAAGCTCGTTGGAA		1370-1390
	qNNV.R2.for	AAATTCAGCCAATGTGCCCC	126	354-374
	qNNV.R2.rev	ATTTGGCAACGACTGCACCA		460-480
RNA-ISH	ISH.R1.for	GGCAAGTGTTACGCTCGTGA	462	1299-1319
	ISH.R1.rev	CGTTGGCATGTACCACGGAA		1741-1761
	ISH.R2.for	ACCTGGTCGGCTGATACTCC	444	562-582
	ISH.R2.rev	ACAGGCAGCAGGATTTGACG		986-1006

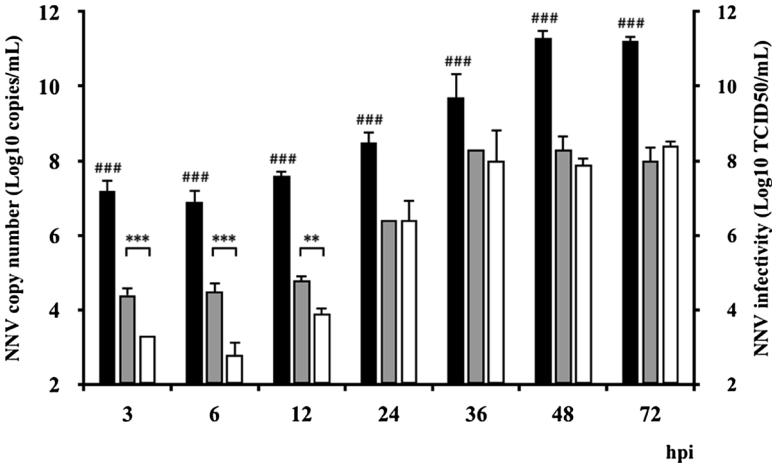

Fig. 1. Expression of viral genomic segment and NNV infectivity in SSN-1 cell at different times post-infection. Levels of RNA1 and RNA2 were determined by qRT-PCR. NNV infectivity was determined as $TCID_{50}$ in SSN-1 cells. Black, gray and white represent RNA1, RNA2, and NNV infectivity, respectively. Error bar indicates standard deviations of the means ($n = 3$). Asterisks indicate significant differences (** $p < 0.01$ and *** $p < 0.001$). The hash symbols ($^{###}$) indicate significant differences from RNA2 segment and NNV infectivity groups ($p < 0.001$).

Table 2
NNV detection by RNA-ISH and ICC in SSN-1 cells at 72 h post inoculation.

Detection tools		Time post inoculation (hours)						
		3	6	12	24	36	48	72
RNA-ISH	RNA1	–[a]	–	+	+ +	+ +	+ +	+ + +
	RNA2	–	–/+	+	+	+ +	+ +	+ + +
ICC		NT	NT	–	–/+	+	+ +	+ + +

[a] Staining intensity: (–) no signal; (–/+) weakly; (+) lowly; (+ +) moderately; (+ + +) highly; (NT) not tested.

2.7. Immunocytochemistry (ICC)

The purification of NNV particles was carried out as described previously (Kim et al., 2018). Monoclonal antiserum was developed in BALB/c mice inoculated with purified NNV, Briefly, purified NNV was mixed with an equal volume of complete Freund`s adjuvant (Gibco) and intraperitoneally (IP) injected into BALB/c mice following the protocol previously described by Gye et al. (2018). Immunized spleen cells were fused with mouse myeloma cells (SP2/0-Ag14) using polyethylene glycol (Roche) followed by selection with hypoxanthine-aminopterin-thymidine (HAT). Hybridoma reacting with purified NNV was selected and used for experiments.

For the detection of viral particles, formalin fixed slides were rehydrated in a graded series of methanol and subjected to heat-induced epitope retrieval (HIER) in 0.01 M citrate buffer (pH 6.0) for 10 min in a microwave. Peroxidase activity was then blocked by incubating slides with 3% H_2O_2 for 10 min at room temperature. After washing in PBS for 5 min, non-specific proteins were blocked by incubating with 10% normal goat serum (Cell Signaling Technology) at room temperature for 30 min. Following the blocking step, slides were incubated with anti-RGNNV monoclonal antibody (1:10 dilution in PBS) for 1 h and washed 4 times with PBS for 5 min each. Slides were then incubated with 1:500 dilution of goat anti-mouse IgG horseradish peroxidase (HRP) conjugated (AB Frontier) in PBS for 1 h. The colorimetric detection was performed using a 3.3`–diaminobenzidine (DAB) substrate kit (Abcam) according to the manufacturer`s instructions. After reacting at room temperature for 10 min, the color reaction was stopped by adding PBS. Slides were mounted and photographed as described above.

3. Results

3.1. Viral replication in NNV-infected SSN-1 cells

NNV replication curves according to viral copy number of RNA1 and RNA2 by qRT-PCR and NNV infectivity by $TCID_{50}$/mL values are shown in Fig. 1. After inoculation, RNA1 replication in cells remained at $< 10^{7.2}$ copies/mL until 6 hpi, after which there was a continual increase in copy numbers with $10^{7.6}$, $10^{8.5}$, $10^{9.7}$, $10^{11.3}$, and $10^{11.2}$ copies/mL at 12, 24, 36, 48, and 72 hpi, respectively. RNA2 in cells was also maintained at a lower level ($< 10^{4.5}$ copies/mL) until 6 hpi, with subsequent increase from 12 to 24 hpi ($10^{4.8}$ and $10^{6.4}$ copies/mL), and higher copy number was observed at 36–72 hpi with over $10^{8.1}$ copies/mL. The titer of NNV in cells ranged between $10^{3.3}$ and $10^{8.4}$ $TCID_{50}$/mL, with a significant increase from 12 to 48 hpi, and reaching highest values at 72 hpi.

The gene expression of RNA1 at each time point was significantly different from that in RNA2 and viral infectivity. By contrast, the expression of RNA2 genes and viral infectivity was significantly different at 3–12 hpi with no significant differences after 24 hpi.

3.2. RNA in situ hybridization (RNA-ISH) and immunocytochemistry (ICC)

To detect viral infection in SSN-1 cells after inoculation of NNV, formalin-fixed slides were subjected to RNA-ISH or ICC. Both RNA segments were detected by ISH using fluorescein and digoxigenin RNA probes. NNV coat protein was investigated by ICC staining. Viral genome was detected by RNA-ISH at 6 hpi, although only the RNA2 segment was only weakly detected (Table 2). Afterwards, two viral RNA genes were clearly detected at 12 hpi, and the intensity of the signal

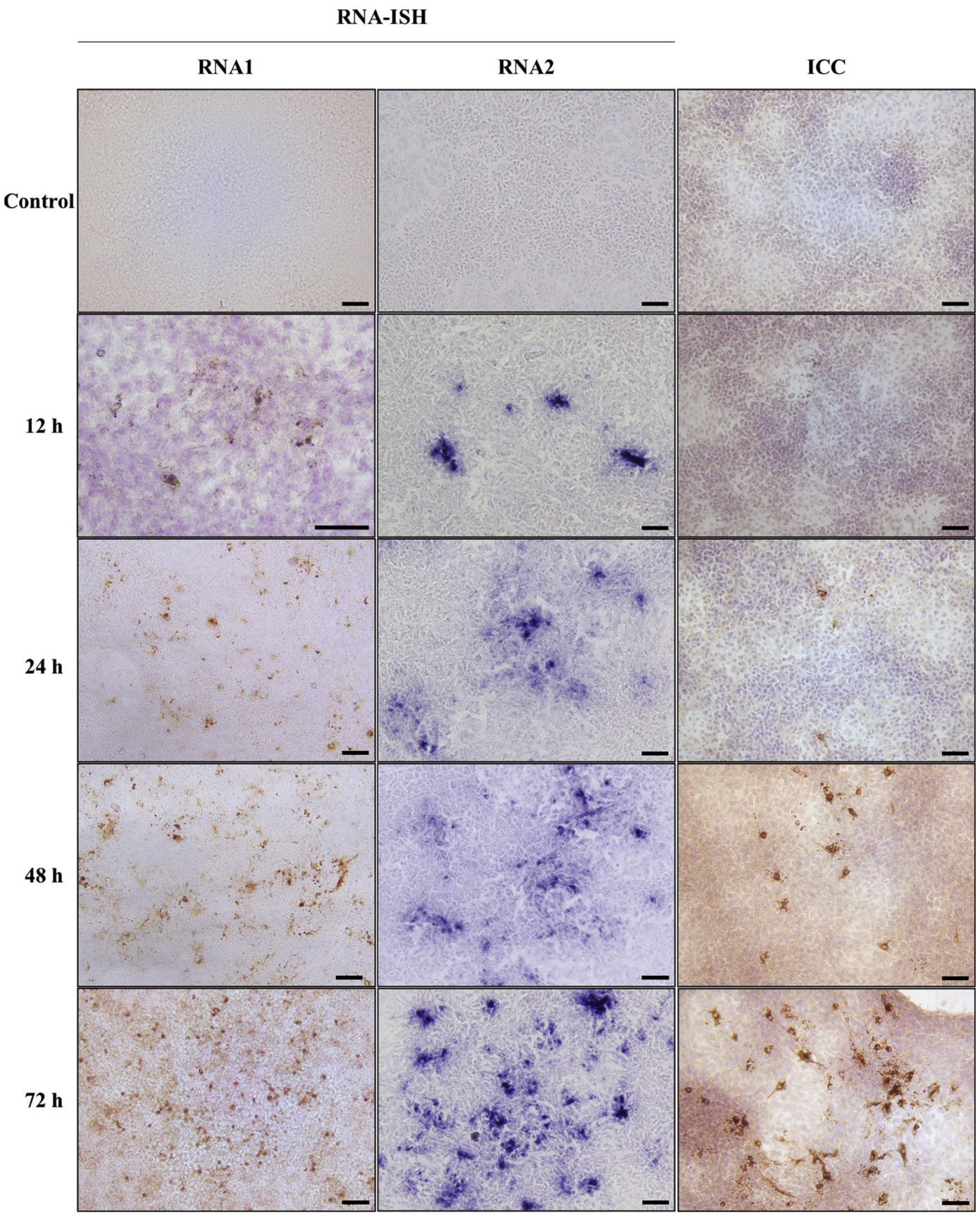

Fig. 2. RNA-ISH and IHC results from NNV-infected SSN-1 cells. Cell slides were processed at 12, 24, 48, and 72 hpi. RNA1 segment was detected using fluorescein RNA probe (orange color). RNA2 segment was examined through DIG RNA probe (blue color). NNV coat protein was detected using anti-RGNNV monoclonal antibody. Positive cells contain brown signals. No signal was detected from non-infected cells. Bar represents 50 μm (For interpretation of the references to colour in this figure legend, the reader is referred to the web version of this article).

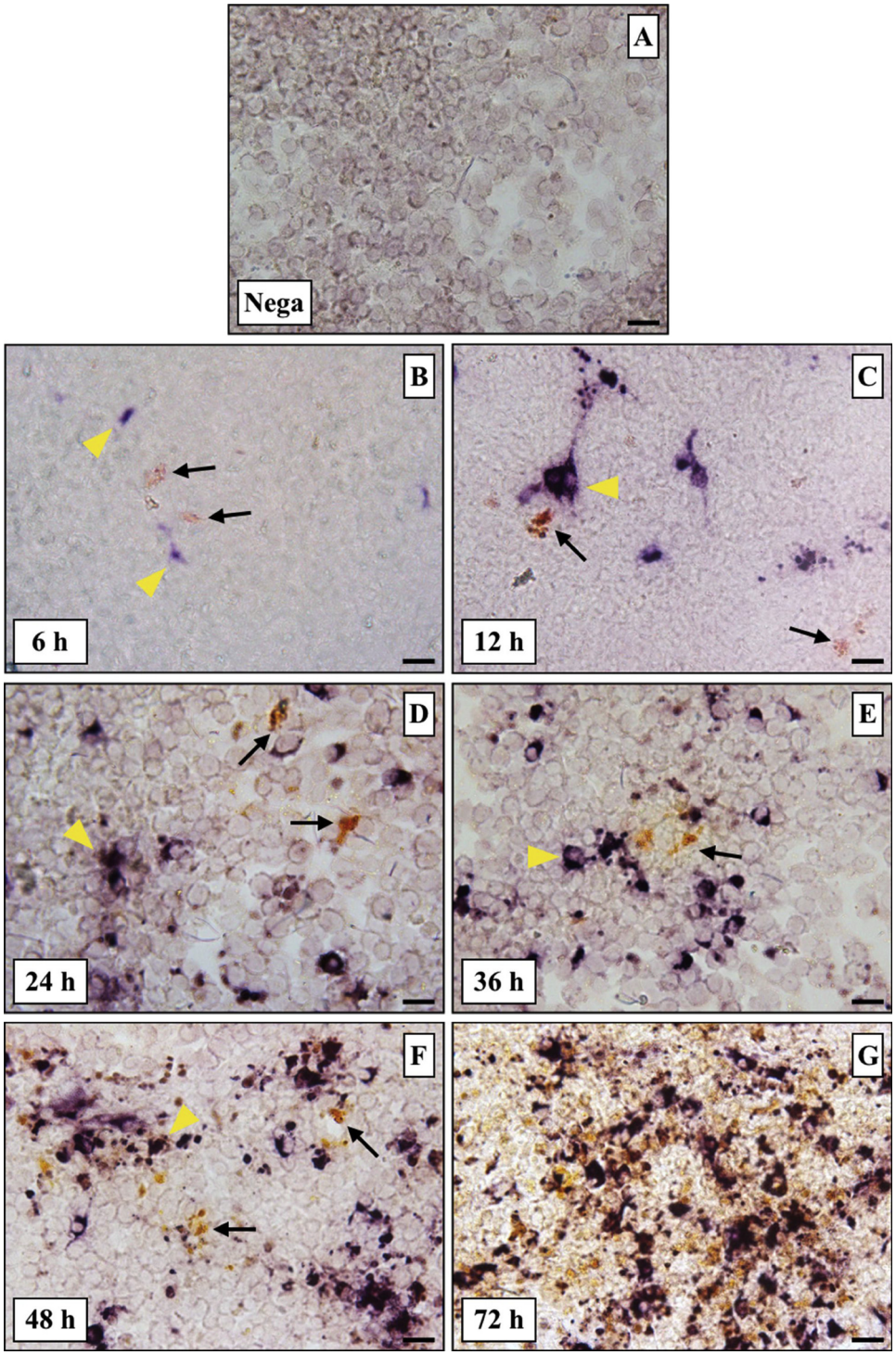

Fig. 3. Double labeling *in situ* hybridization with RNA probe coding for RNA1 and RNA2 in NNV-infected SSN-1 cells. Cell slides were processed at 6 hpi (B), 12 hpi (C), 24 hpi (D), 36 hpi (E), 48 hpi (F) and 72 hpi (G). The presence of separately expressed RNA1 segment (black arrows) and co-expressed RNA1 and RNA2 (yellow arrow heads). Negative control cells (A) were not detected. Bar represents 20 μm (For interpretation of the references to colour in this figure legend, the reader is referred to the web version of this article).

was significantly greater from 24 to 48 hpi (Fig. 2). The highest intensity of the signal was recorded at 72 hpi. As for the signal detection by ICC, viral proteins were first detected at 24 hpi (Fig. 2). Sampled cell slides showed sporadically distributed positive signals until 36 hpi, but signal intensity increased at 48 and 72 hpi.

3.3. Two-color visualization by double labeling RNA-ISH

Double RNA labeling ISH was performed using antisense RNA probes specific for RNA1 and RNA2 segments of NNV. These specific labeled probes of RNA1 and RNA2 were stained with INT/BCIP (orange) and NBT/BCIP (blue), respectively. RNA1 segments were first observed at 6 hpi, although the intensity of the signal was weak (Fig. 3B). Moreover, both specific RNA probes were detected, with the

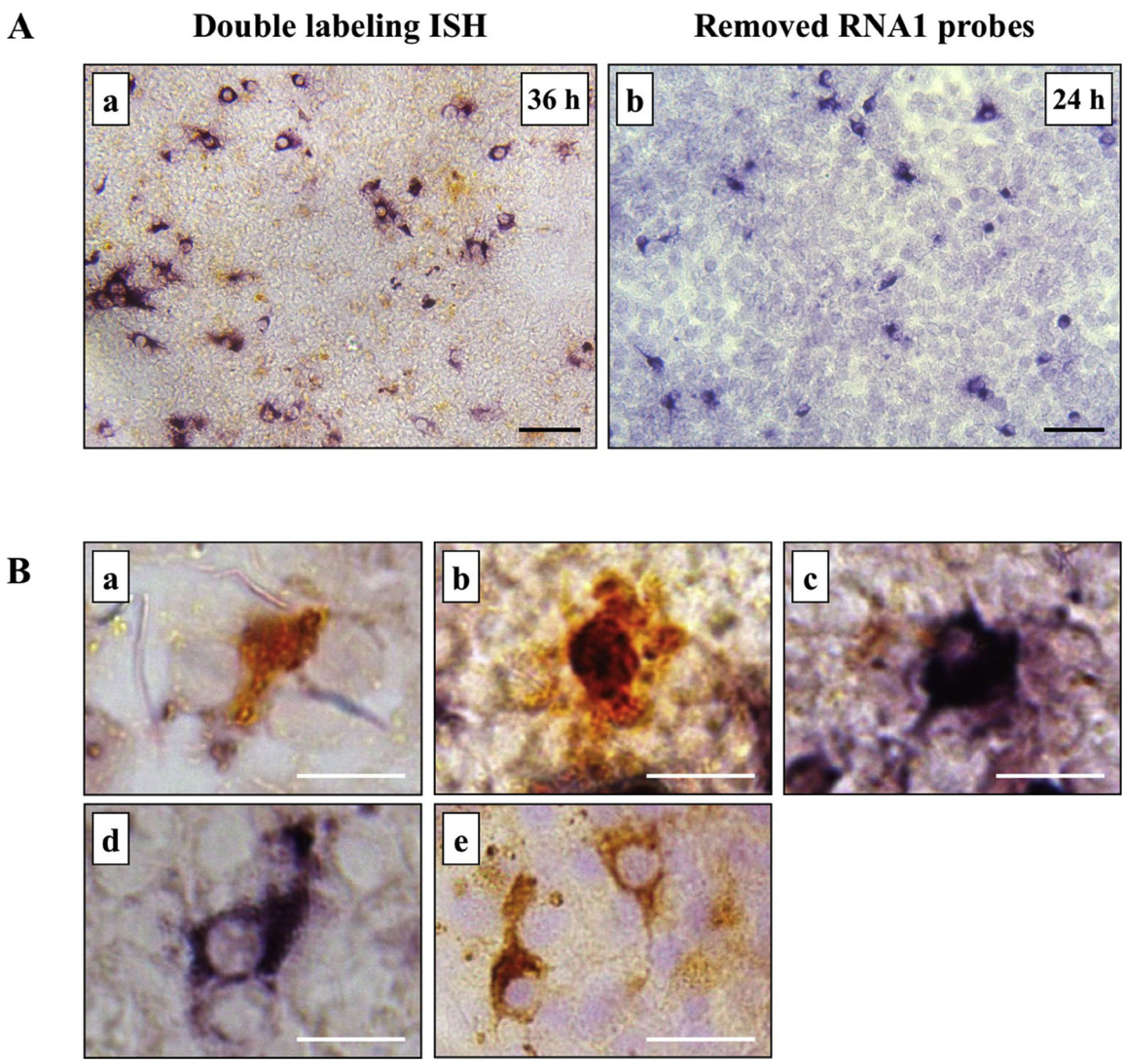

Fig. 4. RNA1 is widely distributed in cells and NNV staining pattern by double labeling ISH. (A) Comparison of double labeling ISH at 36 hpi (a) and double labeling ISH with removed RNA1 probe at 24 hpi (b). (B) The viral genomic segments were stained with various patterns, such as RNA1 expressed only (a), sporadic coexpression of two segments (b) and fully co-expression (c and d), which gives a similar pattern of staining to ICC (e). Bar represent 50 μm (A) and 20 μm (B).

colors combined from INT/BCIP and NBT/BCIP to yield purple. This indicated that co-existence of RNA1 and RNA2 genes in the same regions in cells. At 12 hpi, combined color intensity was more than at 6 hpi, and the RNA1 gene was clearly detected (Fig. 3C). The number of stained viral genomic segments was significantly increased at 24–48 hpi (Fig. 3D, 4 E-F). The highest intensity of the signal was detected at 72 hpi (Fig. 3G).

The RNA1 signal was stronger and/or more widely distributed with increasing time after infection. To confirm separate expression of RNA1 or co-expression of RNA1 and RNA2, the RNA1 probe used for staining was removed using alcohol after double labeling-ISH (Fig. 4A). RNA2 only localized in cells without RNA1 (Fig. 4A, b). Moreover, RNA2 stained blue. These results indicated that labeling was specific and RNA1 gene was expressed at a higher level than RNA2.

Based on the visualization of the two-color viral genomic segments RNA1 and RNA2, the staining pattern was judged to be diverse in NNV-infected cells (Figs. 4B). Various patterns of staining were observed, and included the RNA1 segment stained orange (Fig. 4B, a), staining as purple dots in the RNA1 signal region (Fig. 4B, b), intense purple staining of both RNA segments (Fig. 4B, c), and purple staining of both RNA segments exterior to the cells (Fig. 4B, d), which was very similar to the coat protein staining with ICC (Fig. 4B, e).

4. Discussion

The RNA1 copy number was significantly higher than that of RNA2 or NNV infectivity in all tested samples. RNA1 encodes an RdRp, which has various crucial roles important for production of viral RNA templates, assembly of viral RNA, and activation of RNA synthesis (Ahlquist, 2002). These results suggest the involvement of the RNA1 segment in the early stage of NNV replication, as previously reported by Kim et al. (2018b). The RNA2 segment was also expressed at a higher level than infectivity titer until 12 hpi. However, gene expression of RNA2 and viral infectivity after 24 hpi did not differ significantly. These results might explain the relationship between RNA2 replication and NNV particle. Protein α is the precursor of NNV coat protein and is important for viral infection which might trigger an internal death signal of cells to induce apoptosis (Guo et al., 2003). Wu et al. (2008) reported that protein α induces the loss of mitochondrial membrane permeabilization, which typically precedes signs of necrosis and cytochrome *c* release while later stage protein α always triggers post-apoptotic necrosis cell death. Thus, these results suggest RNA1 might be expressed soon after cells become infected. This could be followed by RNA2 expression to induce apoptosis or necrosis cell death, which leads to increased packaging of infectious particles after 24 hpi.

NNV genomic segments RNA1 and RNA2 were detected within 12 hpi in infected cells using RNA-ISH, while they were detected at 24 hpi by ICC. Although the RNA-ISH method seems to be better than the ICC method for the detection of NNV in infected cells, and may explain the completion of protein production and viral assembly processes, because the ISH protocol is based on viral mRNA detection while ICC is based on antigen (protein) detection. Copy numbers of RNA1 and RNA2 segments were almost unchanged until 12 hpi but subsequently increased along with their infectivity titer at 24 hpi. The inoculated cells displayed partial CPE after 36 hpi, with extensive CPE was observed at 72 hpi (data not shown). This suggests that RNA1 and RNA2 might replicate or be expressed at an early stage (ISH detection within 12 hpi) in the absence of viral antigens. Virions (ICC detection after 24 hpi) are then assembled through the initially expressed viral genomic segments. The assembled NNV begins to infect the cells, which leads to cell death. These findings support the RNA-ISH and ICC as valuable tools for viral detection and for viral infection mechanism studies.

This is the first study visualizing NNV by double labeling ISH following time dependent manner in NNV-infected cells. The coloration of two viral genomic segments (RNA1 and RNA2) was clearly seen in infected SSN-1 cells. Double labeling RNA-ISH revealed these two viral genomic segments in the same region of cells. The purple color was the combined color of the two probes, which was clearly different from the orange color due to INT/BCIP staining of the RNA1 segment and the blue color due to NBT/BCIP staining of the RNA2 segment. The results observed were similar to our previous study (Kim et al., 2018a) showing a dark purple color for co-expression in NNV-infected cells. Moreover, Nørgaard Hansen et al., (2000) detected five pre-prohormones mRNA in *Hydra magnipapillata* using double labeling ISH. The author described the co-existence of two different genes in the same peduncle neurons with combined color. Thus, the combined color indicates that RNA1 and RNA2 segments are co-expressed in infected cells and might represent partial or complete NNV. In addition to the combined color, the RNA1 gene was also expressed separately. The intensity of the RNA1 signal also increased as the combined signal intensity increased. These results provide evidence that the copy number of RNA1 is always higher than that of the RNA2 segment, and suggest that RNA1 over-expression may be important for sufficient assembly of infectious particles as discussed earlier.

NNV segments were first detected at 6 hpi by RNA-ISH using single double labeling. Although the signal detection by ISH correlated with qRT-PCR results as the signal intensified with time, it was less sensitive at early time points than qRT-PCR. The results agree with the descriptions by Lopez-Jimeha et al. (2011) and Corbeil et al. (2015). However, qRT-PCR is not sufficient to localize and visualize the viral segments *in situ*, which underlines the value of the RNA-ISH assay.

Guo et al. (2004) reported that protein A alone was sufficient for cytoplasm localization in the absence of capsid proteins. Moreover, Wu et al. (2010) found that RdRp is an early protein and capsid is a late protein alone with decreased level of RdRp protein. In this study, we found various patterns of staining using double labeling RNA-ISH: (i) expressed RNA1 gene only, (ii) co-expression of two viral genomic segments in the same region of the cell, with the expression of RNA2 being less than that of RNA1, (iii) full co-expression of the two viral genomic segments; and (iv) co-expression of two viral genomic segments in cell outer membrane. These observations were similar to the various staining patterns of coat protein stained by ICC using NNV specific antigen. These results might reflect that some, if not all, RNA1 is localized in the cytoplasm (the site of mitochondria) and expressed earlier than RNA2, while RNA2 is expressed after RNA1 expression to assemble the protein, with RNA1 expression decreased in the co-existing segments. Finally, RNA replication complexes are located at the outer membrane.

In summary, RNA1 is expressed early in contrast to RNA2 segment during NNV replication process. Virions are then assembled initially through expressed viral genomic segments. Although the packaging of infectious particles is efficient, RNA1 is still over-produced. Thus, RNA1 might contribute to the assembly of huge number of viral particles early during NNV replication. Localization of NNV segments by ISH will be useful for understanding the viral infection mechanism or viral replication and providing the answer to control the spread of virus.

Acknowledgement

The research was supported by a grant (2018R1D1A1B07041277) from the National Research Foundation (NRF) funded by the Ministry of Education, Science and Technology (MEST), Republic of Korea.

References

Ahlquist, P., 2002. RNA-dependent RNA polymerases, viruses, and RNA silencing. Science 296, 1270–1273. https://doi.org/10.1126/science.1069132.

Cha, S.J., Do, J.W., Lee, N.S., An, E.J., Kim, Y.C., Kim, J.W., Park, J.W., 2007. Phylogenetic analysis of betanodaviruses isolated from cultured fish in Korea. Dis. Aquat. Org. 77, 181–189. https://doi.org/10.3354/dao01840.

Chi, S.C., Lo, B.J., Lin, S.C., 2001. Characterization of grouper nervous necrosis virus (GNNV). J. Fish Dis. 24, 3–13. https://doi.org/10.1046/j.1365-2761.2001.00256.x.

Comps, M., Trindade, M., Delsert, C., 1996. Investigation of fish encephalitis viruses (FEV) expression in marine fishes using DIG-labelled probes. Aquaculture 143, 113–121. https://doi.org/10.1016/0044-8486(96)01264-1.

Corbeil, S., Faury, N., Segarra, A., Renault, T., 2015. Development of an in situ hybridization assay for the detection of ostreid herpesvirus type 1 mRNAs in the Pacific oyster, *Crassostrea gigas*. J. Virol. Methods 211, 43–50. https://doi.org/10.1016/j.jviromet.2014.10.007.

Costa, J.Z., Thompson, K.D., 2016. Understanding the interaction between Betanodavirus and its host for the development of prophylactic measures for viral encephalopathy and retinopathy. Fish Shellfish Immunol. https://doi.org/10.1016/j.fsi.2016.03.033.

David, R., Tréguier, C., Montagnani, C., Belliard, C., Levy, P., Nédélec, G., Joufoques, V., Remoissenet, G., Gueguen, Y., Cochennec-Laureau, N., 2010. Molecular detection of betanodavirus from the farmed fish, *Platax orbicularis*(Forsskal) (Ephippidae), in French Polynesia. J. Fish Dis. 33, 451–454. https://doi.org/10.1111/j.1365-2761.2009.01136.x.

Frerichs, G.N., Rodger, H.D., Peric, Z., 1996. Cell Culture Isolation of Piscine Neuropathy Nodavirus from Juvenile Sea Bass, *Dicentrarchus labrax*. J. Gen. Virol. 77, 2067–2071. https://doi.org/10.1099/0022-1317-77-9-2067.

Grove, S., Faller, R., Soleim, K.B., Dannevig, B.H., 2006. Absolute quantitation of RNA by a competitive real-time RT-PCR method using piscine nodavirus as a model. J. Virol. Methods 132, 104–112. https://doi.org/10.1016/j.jviromet.2005.08.022.

Guo, Y.X., Wei, T., Dallmann, K., Kwang, J., 2003. Induction of caspase-dependent apoptosis by betanodaviruses GGNNV and demonstration of protein alpha as an apoptosis inducer. Virology 308, 74–82.

Guo, Y.X., Chan, S.-W., Kwang, J., 2004. Membrane association of greasy grouper nervous necrosis virus protein A and characterization of its mitochondrial localization targeting signal. J. Virol. 78, 6498–6508. https://doi.org/10.1128/JVI.78.12.6498-6508.2004.

Gye, H.J., Park, M.-J., Kim, W.-S., Oh, M.-J., Nishizawa, T., 2018. Heat-denaturation of conformational structures on nervous necrosis virus for generating neutralization antibodies. Aquaculture 484, 65–70. https://doi.org/10.1016/j.aquaculture.2017.10.034.

Johansen, R., Sommerset, I., Torud, B., Korsnes, K., Hjortaas, M.J., Nilsen, F., Nerland, A.H., Dannevig, B.H., 2004. Characterization of nodavirus and viral encephalopathy and retinopathy in farmed turbot, Scophthalmus maximus (L.). J. Fish Dis. 27, 591–601. https://doi.org/10.1111/j.1365-2761.2004.00581.x.

Kim, Jong-Oh, Kim, W.-S., Cho, J.-K., Kim, K.-M., Son, M.-H., Oh, M.-J., 2014. Complete genome sequence of nervous necrosis virus isolated from sevenband grouper (*Epinephelus septemfasciatus*) in South Korea. Genome Announc. 2https://doi.org/10.1128/genomeA.01264-14. e01264–14–e01264–14.

Kim, Wi-Sik, Kim, S.-W., Oh, M.-J., 2018. Production of monoclonal antibodies against nervous necrosis virus (NNV, RGNNV genotype). J. Korean Fish. Soc. 51 (3), 328–331. https://doi.org/10.5657/KFAS.2018.0328.

Kim, Jae-Ok, Kim, J.-O., Kim, S.-J., Kim, W.-S., Oh, M.-J., 2018a. Development of double labeling in situ hybridization using RNA probes for genome detection of nervous necrosis virus (NNV). Mol. Cell. Probes 42, 18–24. https://doi.org/10.1016/j.mcp.2018.10.003.

Kim, Jae-Ok, Kim, S.-J., Kim, J.-O., Kim, W.-S., Oh, M.-J., 2018b. Distribution of nervous necrosis virus (NNV) in infected sevenband grouper, *Hyporthodus septemfasciatus* by intramuscular injection or immersion challenge. Aquaculture 489, 1–8. https://doi.org/10.1016/j.aquaculture.2018.01.042.

Kumar, A., 2010. In situ hybridization. Int. J. Appl. Biol. Pharm. 1, 418–430.

Lopez-Jimena, B., Alonso, M.D.C., Thompson, K.D., Adams, A., Infante, C., Castro, D., Borrego, J.J., Garcia-Rosado, E., 2011. Tissue distribution of Red Spotted Grouper Nervous Necrosis Virus (RGNNV) genome in experimentally infected juvenile European seabass (*Dicentrarchus labrax*). Vet. Microbiol. 154, 86–95. https://doi.org/10.1016/j.vetmic.2011.06.029.

Mézeth, K.B., Patel, S., Henriksen, H., Szilvay, A.M., Nerland, A.H., 2009. B2 protein from betanodavirus is expressed in recently infected but not in chronically infected fish. Dis. Aquat. Org. 83, 97–103. https://doi.org/10.3354/dao02015.

Mori, K.-I., Nakai, T., Muroga, K., Arimoto, M., Mushiake, K., Furusawa, I., 1992. Properties of a new virus belonging to nodaviridae found in larval striped jack (*Pseudocaranx dentex*) with nervous necrosis. Virology 187, 368–371. https://doi.org/10.1016/0042-6822(92)90329-N.

Munday, B.L., Kwang, J., Moody, N., 2002. Betanodavirus infections of teleost fish: a review. J. Fish Dis. 25, 127–142. https://doi.org/10.1046/j.1365-2761.2002.00350.x.

Nakai, T., Sugaya, T., Nishioka, T., Mushiake, K., 2009. Current Knowledge on Viral Nervous Necrosis (VNN) and Its Causative Betanodaviruses. https://doi.org/10.15242/iicbe.c1215021.

Nishizawa, T., Mori, K.I., Furuhashi, M., Nakai, T., Furusawa, I., Muroga, K., 1995. Comparison of the coat protein genes of five fish nodaviruses, the causative agents of viral nervous necrosis in marine fish. J. Gen. Virol. 76, 1563–1569. https://doi.org/10.1099/0022-1317-76-7-1563.

Nørgaard Hansen, G., Williamson, M., Grimmelikhuijzen, C.J.P., 2000. Two-color double-labeling in situ hybridization of whole-mount Hydra using RNA probes for five different Hydra neuropeptide preprohormones: evidence for colocalization. Cell Tissue Res. 301, 245–253. https://doi.org/10.1007/s004410000240.

Nopadon, P., Aranya, P., Tipaporn, T., Toshihiro, N., Takayuki, K., Masashi, M., Makoto, E., 2009. Nodavirus associated with pathological changes in adult spotted coral-groupers (*Plectropomus maculatus*) in Thailand with viral nervous necrosis. Res. Vet. Sci. 87, 97–101. https://doi.org/10.1016/j.rvsc.2009.01.004.

Olveira, J.G., Souto, S., Dopazo, C.P., Thiery, R., Barja, J.L., Bandin, I., 2009. Comparative analysis of both genomic segments of betanodaviruses isolated from epizootic outbreaks in farmed fish species provides evidence for genetic reassortment. J. Gen. Virol. 90, 2940–2951. https://doi.org/10.1099/vir.0.013912-0.

Reed, L.J., Muench, H., 1938. A simple method of estimating fifty per cent endpoints. Am. J. Epidemiol. 27, 493–497. https://doi.org/10.1093/oxfordjournals.aje.a118408.

Rodriguez Saint-Jean, S., Borrego, J.J., Perez-Prieto, S.I., 2003. Infectious pancreatic necrosis virus: biology, pathogenesis, and diagnostic methods. Adv. Virus Res. 62, 113–165.

Sommerset, I., Nerland, A.H., 2004. Complete sequence of RNA1 and subgenomic RNA3 of Atlantic halibut nodavirus (AHNV). Dis. Aquat. Org. 58, 117–125. https://doi.org/10.3354/dao058117.

Wu, H.-C., Chiu, C.-S., Wu, J.-L., Gong, H.-Y., Chen, M.-C., Lu, M.-W., Hong, J.-R., 2008. Zebrafish anti-apoptotic protein zfBcl-xL can block betanodavirus protein alpha-induced mitochondria-mediated secondary necrosis cell death. Fish Shellfish Immunol. 24, 436–449. https://doi.org/10.1016/j.fsi.2008.01.001.

Wu, Y.-C., Lu, Y.-F., Chi, S.-C., 2010. Anti-viral mechanism of barramundi Mx against betanodavirus involves the inhibition of viral RNA synthesis through the interference of RdRp. Fish Shellfish Immunol. 28, 467–475. https://doi.org/10.1016/j.fsi.2009.12.008.